New Semiconductor Materials and Devices for Terahertz Imaging and Sensing

T. Otsuji, T. Watanabe, K. Akagawa, Y. Tanimoto,
S. Boubanga Tombet, T. Suemitsu
RIEC: Research Institute of Electrical Communication
Tohoku University
Sendai, Japan
otsuji@riec.tohoku.ac.jp

S. Chan
Nano-Japan Rice University and Tohoku University
University of Pennsylvania
Sendai, Japan
Philadelphia, USA
silviach@seas.upenn.edu

D. Coquillat, W. Knap
GES: Groupe d'Etdue de Semiconduecteurs
CNRS, Universit´e Montpellier 2
Montpellier, France
dominique.coquillat@univ-montp2.fr

V. Ryzhii
CNEL: Computer Nano-Electronics Laboratory,
University of Aizu
Aizu-Wakamatsu, Japan
v-ryzhii@u-aizu.ac.jp

***Abstract*— Recent advances in materials and device structures for terahertz imaging and sensing technology are reviewed. The fundamental physical principle for terahertz imaging/sensing is focused on the nonlinear dynamics of plasmons in two-dimensional semiconductors including quantum wells in III-V based heterostructures as well as graphene.**

I. INTRODUCTION

In the research of modern terahertz (THz) electronics, development of compact, tunable and coherent sources/ detectors operating at THz frequencies is one of the hottest issues. Two-dimensional (2D) plasmons in semiconductor devices like a high electron mobility transistor (HEMT) using III-V compound semiconductor heterostructures have attracted much attention due to their nature of promoting emission/ detection of electromagnetic radiation in the THz range [1-6]. Plasmon is a quantum of spatio-temporal collective vibration of electron/hole densities whose characteristic frequencies (energies) are quantized. The possibility of the THz detection is due to nonlinear properties of the 2D plasmons, which lead to the rectification of the ac current induced by the incoming THz radiation. As a result, a photoresponse appears in the form of a dc voltage between source and drain which is proportional to the radiation intensity (photovoltaic effect). On the other hand, carbon structures based on monolayers of carbon atoms forming dense honeycomb 2D crystals, namely individual graphene layers (GLs) [7] make promising for different nanoelectronic and optoelectronic device applications. Plasma waves in 2D electron-hole system in GLs controlled by a highly conducting gate are studied theoretically [8, 9]. It is revealed that the gated graphene heterostructures can dramatically improve the performance of voltage tunable terahertz detectors. In this paper recent advances in materials and device structures for terahertz imaging and sensing technology based on the nonlinear dynamics of 2D plasmons are reviewed.

II. THZ IMAGING AND SENSING USING III-V HEMTS

A. Device Fabrication

HEMTs fabricated with GaAs-based heterostructure material systems are frequently utilized for detection/emission of terahertz radiation [3, 4]. To obtain a better responsivity/ sensitivity to THz radiation we introduce InAlAs/InGaAs/InP material systems [10]. An 80-nm gate HEMT fabricated provides a current-gain cutoff frequency 298 GHz and a transconductance 700 mS/mm [11]. The HEMT is subject to 0.3-THz, 2-mW radiation to characterize its detection property. Au ribbon wires for pad-package interconnection can act as antennae. Fig. 1 shows the Vg dependency of photoresponse ΔI_d (the rectification component of the THz radiation in drain current) for various drain bias V_d from 0.5 to 50 mV.

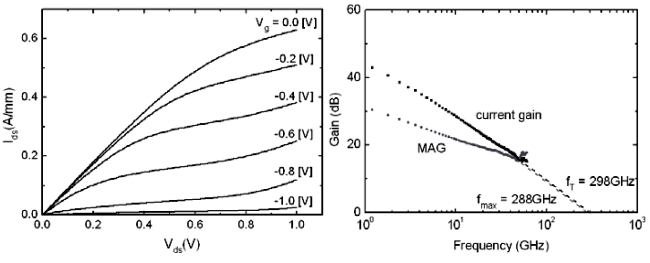

(a) (b)

Figure 1. (a) I-V and (b) f_T characteristics of a 80-nm gate InAlAs/InGaAs/InP HEMT.

978-1-4244-9289-3/11/$26.00 ©2011 IEEE

B. *Experiments for THz Imaging and Sensing*

First the detection sensitivity of the HEMT was evaluated [10]. The measurement setup is shown in Fig. 2. For HEMT responsivity measurement, any sample is removed. Typical photoresponse to 292-GHz, 2-mW radiation is plotted in Fig. 3. Intrinsic responsivity without any antenna is estimated to be ~30 V/W. Photocurrent ΔI_d is the rectification component of the THz radiation in the drain current I_d. It is seen that ΔI_d increases proportionally with increase in the drain bias V_d up to -20 mV. However, at higher than 20 mV strong noise is observed. Therefore taking into account of the better S/N condition we choose V_d = 2 mV for the imaging. The gate bias V_g is fixed at −0.87 V where ΔI_d becomes the maximum.

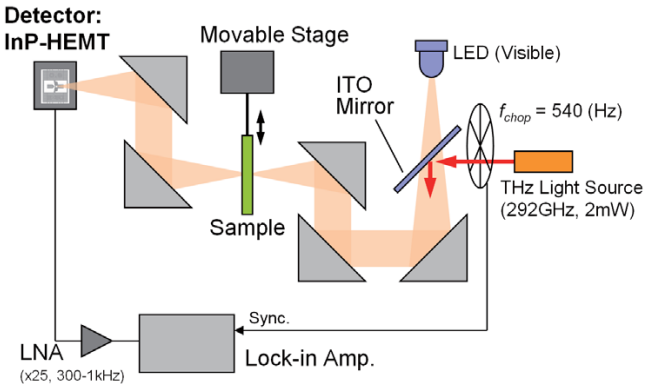

Figure 2. THz imaging system instrumentation.

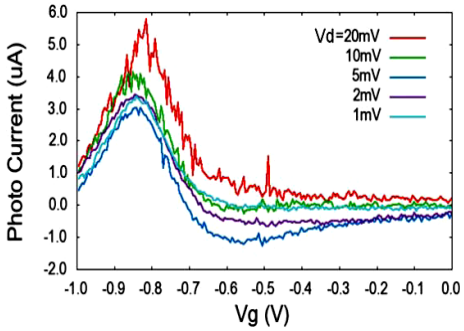

Figure 3. Photoresponse of the HEMT to the 0.3-THz, 2-mW radiation.

We performed raster-scan imaging in transmission mode with the measurement setup including the HEMT as a detector as shown in Fig. 2 [10]. Typical results are shown in Figs. 4(a)-(d). The samples for the imaging are (a) leaves which are called Acer Monspessulanum (Acer from Montpellier) and Ginkgo Biloba, (b) a tea bag with the package, (c) different kind of tea bags with the packages, and (d) adhesive plasters. From the imaging results shown in Fig. 4(a), the image of the leaves was successfully obtained with good contrast. Regarding the images (b) and (c), the THz radiation transmitted through the packages so that the tea leaves could be identified. The more water contains the more absorbed is the THz radiation, resulting in darker color. The amount of water contained in the tea bags appears in the images (b) and (c) as its darkness. From the image (d), we can recognize the shape of adhesive plasters containing less amount of water than that of the leaves or tea bags.

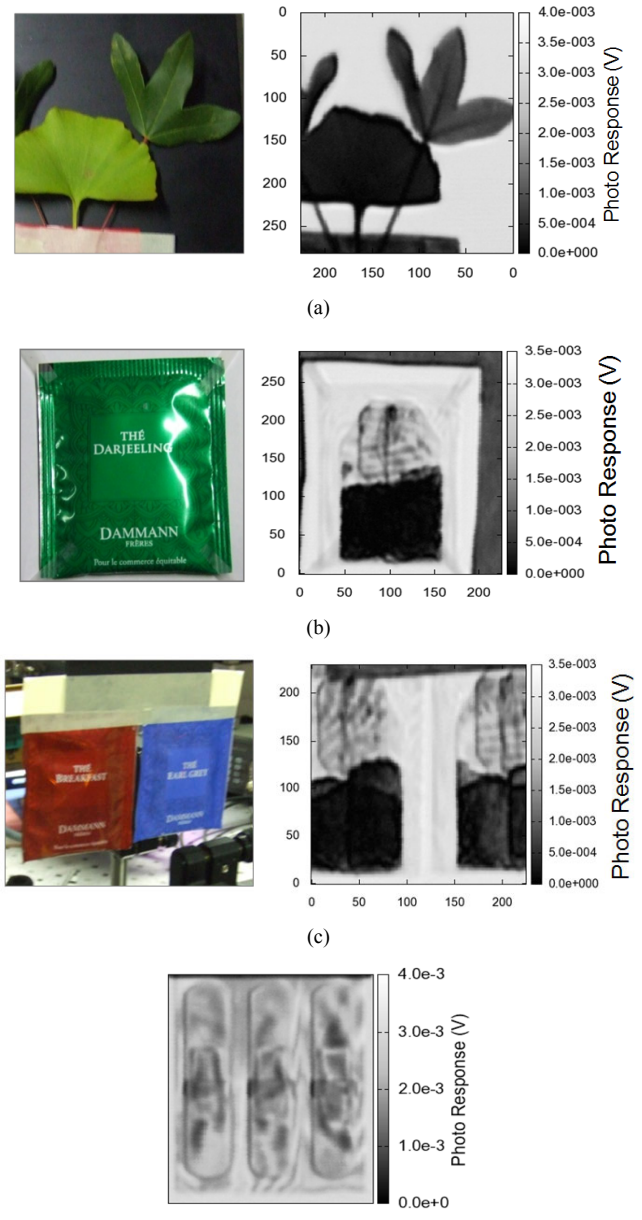

Figure 4. THz imaging results. (a) Acer Monspessulanum and Ginkgo Biloba. Left: photo image, right: THz image. (b) A tea bag. Left: photo image, right: THz image. (c) Different kinds of two tea bags. Left: photo image, right: THz image. (d) Adhesive plasters.

III. Plasmons in Gated Graphene Heterotructures

Recent advances in synthesis (epitaxial growth) of graphene can enable turbostratic (non-chiral) stacking of multiple graphene monolayers than can preserve the energy band structure of monolayer graphene [12, 13]. We call it as individual graphene layers (GLs). We analytically investigated the plasma waves in 2D electron-hole system in GLs

controlled by a highly conducting gate are studied theoretically [8, 9].

We shall consider "classical" plasma waves with the wavelength λ markedly exceeding the characteristic length of the electron de Broglie wave λ_F [8]. In this case, we can use the following kinetic equations coupled with the equation governing the self-consistent electric potential:

$$\frac{\partial f_e}{\partial t} + \boldsymbol{v}_p \frac{\partial f_e}{\partial \boldsymbol{r}} + e\frac{\partial f_e}{\partial \boldsymbol{p}}\frac{\partial \varphi}{\partial \boldsymbol{r}} = I_e, \qquad (1)$$

$$\frac{\partial f_h}{\partial t} + \boldsymbol{v}_p \frac{\partial f_h}{\partial \boldsymbol{r}} - e\frac{\partial f_h}{\partial \boldsymbol{p}}\frac{\partial \varphi}{\partial \boldsymbol{r}} = I_h. \qquad (2)$$

Here $f_e = f_e(\boldsymbol{p},\boldsymbol{r},t)$ and $f_h = f_h(\boldsymbol{p},\boldsymbol{r},t)$ are the electron and hole distribution functions, respectively, $\varphi = (\boldsymbol{r},z,t)$ is the electric potential, $\boldsymbol{p} = (p_x, p_y)$ is the electron (or hole) in-plane momentum, $\boldsymbol{r} = (x,y)$, and e is the elementary charge. The quantity $\boldsymbol{v}_p$ is the velocity of an electron and a hole with momentum $\boldsymbol{p}$: $\boldsymbol{v}_p = \partial\varepsilon_{\boldsymbol{p}}/\partial\boldsymbol{p}$, where $\varepsilon_{\boldsymbol{p}} = v_F|\boldsymbol{p}|$, and v_F is the characteristic (Fermi) velocity. Also, the Poisson equation which supplements Eqs. (1) and (2) is presented as:

$$\frac{\partial^2\varphi}{\partial x^2} + \frac{\partial^2\varphi}{\partial y^2} + \frac{\partial^2\varphi}{\partial z^2} = \frac{4\pi e}{\wp}(n_e - n_h)\delta(z), \qquad (3)$$

where $\wp$ is the permittivity of the surrounding space and $\delta(z)$ is the Dirac delta function playing the role of the form factor of the electron/hole localization normal to the graphene plane.

Using the standard small-signal analysis, we assume that $f_{e,h}(\boldsymbol{p},\boldsymbol{r},t) = f_{e0,h0}(p) + \delta f_{e,h}(p)\exp[i(kx-\omega t)]$ and $\varphi(\boldsymbol{r},z,t) = \delta\varphi(z)\exp[i(kx-\omega t)]$, where $|\delta f_{e,h}| << f_{e0,h0}$ are small perturbations, k and ω are the wave number and angular frequency of the plasma wave, respectively. For usual longer plasma waves (k^{-1} is longer than the gate layer thickness d) we derive the dispersion relations for a practical limiting case of relatively low temperatures and/or high gate voltages V_g as follows:

$$\omega = ks \approx kv_F\sqrt{\frac{\alpha}{2}} \equiv kv_F\sqrt{\frac{2e^2\varepsilon_F d}{\wp\hbar^2 v_F^2}} \propto kv_F d^{1/4}V_g^{1/4}. \qquad (4)$$

In this case, the wave phase ω/k and group velocities $\partial\omega/\partial k$ are identical and equal to s.

From Eq. (4) several important aspects of the plasma waves in GLs are seen. First, the plasma wave velocity s is proportional to $V_g^{1/4}$, which is different from the normal semiconductors where $s \propto V_g^{1/2}$. Second, since α >> 1 in a practically wide range of parameters, the plasma wave velocity s is far beyond the Fermi velocity $v_F (\approx 10^8$ cm/s). Compared with normal semiconductors the plasma-wave velocity could be higher by more than one order of magnitude. This makes it possible to implement a THz plasmon resonant cavity in a relaxed dimension of micrometer length L. Since the momentum relaxation time τ of carriers in GLs is quite long (longer than ps even at 300K) compared with those of conventional semiconductors resulting in excellent high quality factors ($\approx s\tau/L$) with relaxed dimensions.

Figure 5 shows calculated quality factors (resonant intensities) of a graphene-channel transistor (GOSFET) at 300K as a function of the gate length (the cavity size) L in comparison with conventional gated semiconductors. It is clearly seen that the graphene exhibits extremely high Q values. This result indicates that the GL based plasmonic devices can surpass the limit on detection sensitivity of conventional semiconductor-based devices.

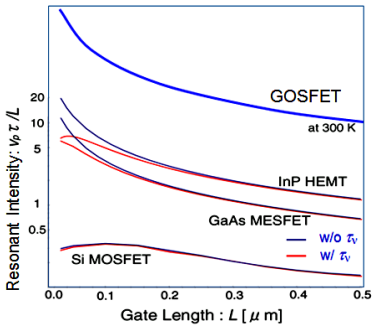

Figure 5. Calculated quality factor (resonant intensity) of gated 2D plasmons in different materials and structures. FET: field effect transistors, HEMT: high electron mobility transistors.

Graphene nanoribbons (GNRs) are possible structures that define characteristic frequencies of 2D plasmons in graphene by the ribbon width, the carrier density, and the incident angle of the THz radiation [9]. We formulated the 2D plasmon dispersion in the gated 2D GNR array:

$$\tilde{\omega}_p = \omega_p - i\gamma = \sqrt{\frac{4\pi e^2 n}{\wp m^*}\frac{q\cos^2\theta}{1+\coth(qd)} - \frac{1}{4\tau^2}} - i\frac{1}{2\tau}, \qquad (5)$$

where γ is the plasmon relaxation rate due to the dissipation in the GNR array, m^* is the electron effective mass in GNR, q is the plasmon wave vector, θ is the angle between the plasmon wave vector (determined by the incident THz radiation) and the GNR direction. Figure 6 shows typical calculated results for the fundamental mode of plasmon frequencies as a function of q for several θ conditions [9].

We have recently experimentally verified such dispersion relations by using optical-pump/terahertz- and optical-probe time-domain spectroscopy. A GNR sample having a 50-μm ribbon width was prepared from an exfoliated graphene on a

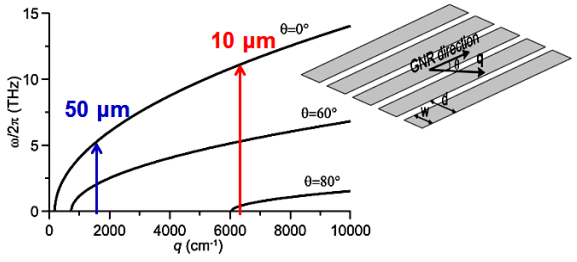

Figure 6. Calculated plasmon frequencies. $m^* = 0.002m_0$, $n = 10^{12}$cm^{-2}, $\nu = 10\times10^{13}$s^{-1} (electron mobility is 36,000 cm2/(Vs)). Crresponding gate lenghts at typical wave vecotors are designated.

SiO2/Si substrate. The sample is optically pumped by a 80-fs, 1550-nm, 2-mW fiber laser pulses with 20-MHz repetition whose polarization is set at $\theta = 0$ deg. The infrared pumping generates excess electrons and holes in conduction and valence band, respectively. The photoelectrons and photoholes will emit optical phonons to relax energies, accumulating around the Dirac point giving rise to population inversion. When the pumping intensity is below the threshold, the dynamic THz conductivity retains in positive [14] so that the 2D plasmon make a distinctive resonant absorption spectra if femtosecond THz impulsive radiation is impinged to the sample during the energy relaxation of photocarriers (ps to 10-ps time scale after the pumping). The temporal response of the THz probe pulse transmitted through the sample was electrooptically detected using a CdTe sensor crystal. Figure 7 shows typical Fourier-transformed spectra. As is expected, the GNR sample exhibits clear absorption peaks corresponding to the 2D plasmon modes. Even though a wide ribbon width of 50 μm sub-THz resonance of the fundamental plasmon mode as high as 450 GHz is observed, demonstrating superiority of the electron transport properties in graphene.

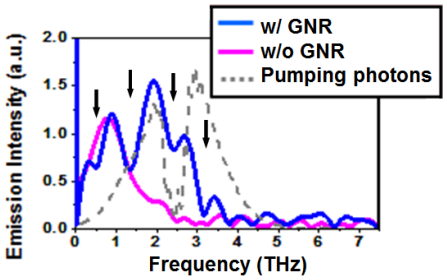

Figure 7. Fourier spectra of a THz probe pulse transmitted through GNR sample under infrared fs-pulsed laser pumping, showing absorption peaks corresponding to the 2D plasmon modes.

IV. Conclusion

Recent advances in 2D-plasmon-related materials and device structures for terahertz imaging and sensing technology were reviewed. Enormous nonlinear dynamics of 2D plasmons and graphene-based new heterostructure materials will revolutionize the THz sensing and imaging technology.

Acknowledgements

This work has been financially supported in part by JSPS GA-SR(S), JSPS-SAKURA, JST-CREST, NSF-PIRE Nano-Japan programs.

References

[1] M. Dyakonov and M. Shur, “Shallow water analogy for a ballistic field effect transistor: New mechanism of plasma wave generation by dc current,” Phys. Rev. Lett. 71, 2465–2468 (1993).

[2] M. Dyakonov and M. Shur, “Detection, mixing, and frequency multiplication of terahertz radiation by two-dimensional electronic fluid,” IEEE Trans. Electron Devices, 43, 380-387 (1996).

[3] W. Knap, M. Dyakonov, D. Coquillat, F. Teppe, N. Dyakonova, J. Lusakowski, K. Karpierz, M. Sakowicz, G. Valusis, D. Seliuta, I. Kasalynas, A. El Fatimy, Y. M. Meziani, and T. Otsuji, "Field effect transistors for terahertz detection: physics and first imaging applications," J. Infrared Milli. Terahz Waves 30, 1319-1337 (2009).

[4] W. Knap, S. Nadar, H. Videlier, S. Boubanga-Tombet, D. Coquillat, N. Dyakonova, F. Teppe, K. Karpierz, J. Łusakowski, M. Sakowicz, I. Kasalynas, D. Seliuta, G. Valusis, T. Otsuji, Y. Meziani, A. El Fatimy, S. Vandenbrouk, K. Madjour, D. Théron, C. Gaquière, "Field Effect Transistors for Terahertz Detection and Emission," J. Infrared Milli. Terahz 32, 618-628 (2011).

[5] T. Otsuji, Y. M. Meziani, T. Nishimura, T. Suemitsu, W. Knap, E. Sano, T. Asano, V.V. Popov, "Emission of terahertz radiation from dual-grating-gates plasmon-resonant emitters fabricated with InGaP/InGaAs/GaAs material systems," J. Phys.: Condens. Matters 20, 384206 (2008).

[6] Y. Tsuda, T. Komori, A. El Fatimy, T. Suemitsu, and T. Otsuji, "Application of plasmonic microchip emitters to broadband terahertz spectroscopic measurement," J. Opt. Soc. Am. B 26, A52-A57 (2009).

[7] A.K. Geim and K.S. Novoselov, “The rise of graphene,” Nature Mat. 6, 183-191 (2007).

[8] V. Ryzhii, A. Satou and T. Otsuji, "Plasma waves in two-dimensional electron-hole system in gated graphene heterostructures," J. Appl. Phys. 101, 024509 (2007).

[9] V. V. Popov, T. Yu. Bagaeva, T. Otsuji, and V. Ryzhii, "Oblique terahertz plasmons in graphene nanoribbon arrays," Phys. Rev. B 81, 073404 (2010).

[10] T. Watanabe, K. Akagawa, Y. Tanimoto, D. Coquillat, W. M. Knap, and T. Otsuji, "Terahertz imaging with InP high-electron-mobility transistors," SPIE Defense, Security & Sensing, Proc. SPIE 8023, 802325 (2011).

[11] Akagawa, K., Fukuda, S., Suemitsu, T., Otsuji, T., Yokohama, H., and Araki, G., “Impact of T-gate electrode on gate capacitance in In0.7Ga0.3As HEMTs,” Phys. Status Solidi C 8, 300-302 (2011).

[12] W.A. de Heer, C. Berger, X. Wu, P.N. First, E.H. Conrad, X. Li, T. Li, M. Sprinkle, J. Hass, M.L. Sadowski, M. Potemski, G. Martinez, "Epitaxial graphene," Solid State Commun. 143, 92-100 (2007).

[13] M. Suemitsu and H. Fukidome, “Epitaxial graphene on silicon substrate,” J. Phys. D: Appl. Phys. 43, 374012 (2010).

[14] V. Ryzhii, M. Ryzhii, and T. Otsuji, "Negative dynamic conductivity of graphene with optical pumping," J. Appl. Phys. 101, 083114 (2007).